Symbolic computation on the multi-soliton-like solutions of the cylindrical Kadomtsev–Petviashvili equation from dusty plasmas

2007 J. Phys. A: Math. Theor. 40 7643

(http://iopscience.iop.org/1751-8121/40/27/014)

IOP PUBLISHING JOURNAL OF PHYSICS A: MATHEMATICAL AND THEORETICAL

J. Phys. A: Math. Theor. **40** (2007) 7643–7657 doi:10.1088/1751-8113/40/27/014

Symbolic computation on the multi-soliton-like solutions of the cylindrical Kadomtsev–Petviashvili equation from dusty plasmas

Juan Li[1], **Hai-Qiang Zhang**[1], **Tao Xu**[1], **Ya-Xing Zhang**[1], **Wei Hu**[2] **and Bo Tian**[1,3,4]

[1] School of Science, Beijing University of Posts and Telecommunications, PO Box 122, Beijing 100876, People's Republic of China
[2] Department of Mathematics and LMIB, Beijing University of Aeronautics and Astronautics, Beijing 100083, People's Republic of China
[3] Key Laboratory of OCLT, Ministry of Education, Beijing University of Posts and Telecommunications, Beijing 100876, People's Republic of China

E-mail: gaoyt@public.bta.net.cn

Received 8 February 2007, in final form 20 April 2007
Published 20 June 2007
Online at stacks.iop.org/JPhysA/40/7643

Abstract
Considering the transverse perturbation and axially non-planar geometry, the cylindrical Kadomtsev–Petviashvili (KP) equation is investigated in this paper, which can describe the propagation of dust-acoustic waves in the dusty plasma with two-temperature ions. Through imposing the decomposition method, such a (2+1)-dimensional equation is decomposed into two variable-coefficient (1+1)-dimensional integrable equations of the same hierarchy. Furthermore, three kinds of Darboux transformations (DTs) for these two (1+1)-dimensional equations are constructed. Via the three DTs obtained, the multi-soliton-like solutions of the cylindrical KP equation are explicitly presented. Especially, the one- and two-parabola-soliton solutions are discussed by several figures and some effects resulting from the physical parameters in the dusty plasma and transverse perturbation are also shown.

PACS numbers: 05.45.Yv, 02.30.Jr, 02.30.Ik, 02.70.Wz

1. Introduction

Owing to the limitation of dimension, the pure one-dimensional models cannot account for all observed features in the auroral region, especially at higher polar altitudes [1–4]. In realistically physical situations, the higher dimensional systems with the transverse perturbation may

[4] Author to whom any correspondence should be addressed.

provide us with the more useful and powerful models as shown in [1–6]. As a typical example in (2+1) dimensions, the Kadomtsev–Petviashvili (KP) equation in a planar geometry with the weakly transverse perturbation has been considerably investigated [7–11]. In fact, a lot of realistic phenomena observed in laboratory devices are not restricted in a planar geometry, but usually in a non-planar geometry [1–6]. Therefore, more and more (2+1)-dimensional models in the non-planar geometry have been derived to describe various nonlinear wave phenomena in an axially symmetric non-planar cylindrical and/or spherical geometry including the evolution of the ring dark soliton in a Bose–Einstein condensate with a thin disc-shaped potential [1], the dust-acoustic wave propagation in a cosmic dusty plasma [2, 3] and the relativistically magnetosonic solitary wave propagating in a collisionless plasma [6].

In the past few decades, extensive attention has been paid to the dynamics of nonlinear dust-acoustic waves in the dusty plasma with two-temperature ions [12–16]. Under the necessary condition $E_R/\omega_{\mathrm{pd}} \ll 1$, the validity of the assumption of two-temperature ions has been verified in various dusty plasma systems including the Saturn's E-ring, noctilucent clouds, Halley's comet and interstellar molecular clouds [12]. In such a consideration, E_R is the energy rate between these two types of ions and ω_{pd} is the characteristic dust plasma frequency of the system determined by $\sqrt{4\pi n_{d0} Z_{d0}^2 e^2 / m_d}$, where n_{d0} is the equilibrium value of the dust particle number density, Z_{d0} is the dust charge number and m_d is the dust mass. As shown in [12–14], it is the small, but finite number density of two-temperature ions that provides the possibility of the coexistence of large amplitude rarefactive or compressive dust-density solitary waves. Meanwhile, the effects of two-temperature ions on the behaviour of dust-acoustic solitary waves have also been discussed in detail [5, 12–16]. Therefore, in order to describe the abundant nonlinear dust-acoustic wave structures in different dusty plasma environments, it is necessary to take the two-temperature ions into account.

In this paper, we would like to investigate a variable-coefficient cylindrical KP equation, which describes the propagation of the two-dimensional dust-acoustic wave in the dusty plasma consisting of cold dust particles, an unmagnified, collisionless, isothermal electrons and two-temperature ions [5, 11–21]. Some one-solitary-wave solutions of this equation have been obtained by using the generalized projected Riccati equation expansion method [5]. Especially, in order to interpret the soliton-like interactions occurring in dusty plasmas, it is necessary to construct the multi-soliton-like solutions. To our knowledge, the investigation on constructing the multi-soliton-like structures for the dust-acoustic waves in such a dusty plasma has not been widespread.

To begin with, let us give a brief retrospect on the derivation of the variable-coefficient cylindrical KP equation from the dusty plasma with two-temperature ions. When the pressure of the dust and two-temperature ions are both considered in the dusty plasma with inertial charged dust fluid and Boltzmann-distributed electrons [5, 11, 15–21], the charge neutrality at equilibrium requires that $n_{\mathrm{il0}} + n_{\mathrm{ih0}} = Z_{d0} n_{d0} + n_{e0}$, where $n_{\mathrm{il0}} (n_{\mathrm{ih0}})$ and n_{e0} are the equilibrium values of unperturbed lower (higher) temperature ion and electron, respectively. The propagation of the two-dimensional dust-acoustic wave in cylindrical geometry is governed by the following system [5, 11–21]:

$$\frac{\partial n_d}{\partial t} + \frac{1}{r}\frac{\partial (r n_d u_d)}{\partial r} + \frac{1}{r}\frac{\partial (n_d v_d)}{\partial \theta} = 0,$$
$$\frac{\partial u_d}{\partial t} + u_d \frac{\partial u_d}{\partial r} + \frac{v_d}{r}\frac{\partial u_d}{\partial \theta} - \frac{v_d^2}{r} = \frac{\partial \psi}{\partial r} - \frac{\varrho}{n_d}\frac{\partial p_d}{\partial r},$$
$$\frac{\partial v_d}{\partial t} + u_d \frac{\partial v_d}{\partial r} + \frac{v_d}{r}\frac{\partial v_d}{\partial \theta} + \frac{v_d u_d}{r} = \frac{1}{r}\frac{\partial \psi}{\partial \theta} - \frac{\varrho}{r n_d}\frac{\partial p_d}{\partial \theta},$$

$$\frac{\partial p_d}{\partial t}+u_d\frac{\partial p_d}{\partial r}+\frac{v_d}{r}\frac{\partial p_d}{\partial\theta}+\gamma_d p_d\left[\frac{1}{r}\frac{\partial(ru_d)}{\partial r}+\frac{1}{r}\frac{\partial v_d}{\partial\theta}\right]=0,$$

$$\frac{1}{r}\frac{\partial}{\partial r}\left(r\frac{\partial\psi}{\partial r}\right)+\frac{1}{r^2}\frac{\partial^2\psi}{\partial\theta^2}=n_d+n_e-n_{\mathrm{il}}-n_{\mathrm{ih}},$$

where r and θ are the radial and polar angle directions, while n_d, p_d and ψ are the number density, pressure of the dust particles and electrostatic potential, respectively. The parameters u_d and v_d represent the velocity components of the dust particles in the r and θ directions. In this case, the variables $t, r, (u_d, v_d), p_d$ and ψ are all normalized by the dust plasma period $\omega_{\mathrm{pd}}^{-1}$, Debye length $\lambda_{Dd}=\sqrt{T_{\mathrm{eff}}/(4\pi e^2 n_{d0}Z_{d0})}$, effective dust-acoustic speed $C_d=\sqrt{Z_{d0}T_{\mathrm{eff}}/m_d}$, $p_{d0}=n_{d0}Z_dT_d$ and T_{eff}/e, respectively. In the above system, $n_e\,(=\nu\,\mathrm{e}^{s\beta_1\psi})$ is the number density of the Boltzmann-distributed electrons with temperature T_e and equilibrium density $\nu\ (=n_{e0}/(Z_dn_{d0}))$, $n_{\mathrm{il}}\,(=\mu_l\,\mathrm{e}^{-s\psi})$ is the density of ion component with low-temperature T_{il} and equilibrium density $\mu_l\,(=n_{\mathrm{il}0}/(Z_dn_{d0}))$, $n_{\mathrm{ih}}\,(=\mu_h\,\mathrm{e}^{-s\beta_2\psi})$ is the density of ion component with high-temperature T_{ih} and equilibrium density $\mu_h\,(=n_{\mathrm{ih}0}/(Z_dn_{d0}))$, $T_{\mathrm{eff}}^{-1}=(n_{e0}/T_e+n_{\mathrm{il}0}/T_{\mathrm{il}}+n_{\mathrm{ih}0}/T_{\mathrm{ih}})/(Z_dn_{d0})$, $\varrho=T_d/T_{\mathrm{eff}}$, $\beta_1=T_{\mathrm{il}}/T_e$, $\beta_2=T_{\mathrm{il}}/T_{\mathrm{ih}}$ and $s=T_{\mathrm{eff}}/T_{\mathrm{il}}$. Through the reductive perturbation method and stretched coordinates as $\xi=\epsilon^{\frac{1}{2}}(r-ct)$, $\eta=\epsilon^{\frac{1}{2}}\theta$ and $\tau=\epsilon^{\frac{3}{2}}t$, where ϵ is a small parameter and c is the phase velocity of waves, the variable-coefficient cylindrical KP equation can be derived as [5, 11–21]

$$-\phi_{\tau\xi}+A\phi_\xi^2+A\phi\phi_{\xi\xi}-D\phi_{\xi\xi\xi\xi}-\frac{1}{2\tau}\phi_\xi-\frac{1}{2c\tau^2}\phi_{\eta\eta}=0. \tag{1}$$

It is worth noting that we here only outline the concise derivation process of equation (1), more details on the physics of dusty plasmas and assumptions in deriving such a model can be seen in [11–21]. In equation (1), ϕ is the first approximation of the dust-acoustic wave potential, $A=\left(\nu\beta_1-\mu_l-\mu_h\beta_2^2+2B^2-\gamma_dB^2+c^2\gamma_dB^3s+c^2B^3s\right)/(2cB^2)$, $D=1/(2cB^2s^2)$, $B=\mu_h\beta_2+\mu_l+\nu\beta_1$ with the equilibrium density of electron component as $\nu=\mu_l+\mu_h-1$. The terms $\phi_\xi/(2\tau)$ and $\phi_{\eta\eta}/(2c\tau^2)$ result from the non-planar cylindrical geometry and the latter also denotes the effect of the transverse perturbation. Actually, equation (1) can also be used to describe the cylindrical nebulon structures in a cosmic dusty plasma environment such as the supernova shells or Saturn's F-ring [2, 22].

This paper is organized as follows. In section 2, through the decomposition method [26–33], equation (2) will be decomposed into two variable-coefficient (1+1)-dimensional integrable nonlinear equations, which are the first two non-trivial equations in the same hierarchy. In section 3, three kinds of Darboux transformations (DTs) will be constructed. In section 4, based on the obtained three DTs, the one-, two-, three- and four-soliton-like solutions of equation (1) will be explicitly presented, and the relevant physical mechanisms will be discussed through the figures for some sample solutions. Section 5 will be our conclusions.

2. Decomposition of equation (2)

It has been demonstrated that by using suitable constraints many higher dimensional integrable systems can be decomposed into two lower dimensional integrable systems [26–33], so that the solutions for the former can be reduced to solve the latter. This also provides a way to investigate the properties of the higher dimensional systems based on the lower dimensional integrable systems. Then, with the help of symbolic computation [24, 25], we will employ the decomposition method to work on equation (1) and construct its multi-soliton-like solutions in this paper.

For simplicity, equation (1) can be rewritten into its equivalent form

$$(u_t + 6uu_x + u_{xxx})_x + \frac{1}{2t}u_x + \frac{\sigma^2}{t^2}u_{yy} = 0 \tag{2}$$

by the scaling transformation

$$\phi = -\frac{6D}{A}u(x, y, t), \quad x = \xi, \quad y = \pm\sqrt{\frac{2c}{D}}\sigma\eta, \quad t = D\tau, \tag{3}$$

where x and y are the scaled 'space' and t is the scaled 'time', while $\sigma = \pm 1$.

By the decomposition, the investigation on equation (2) will be reduced to deal with two variable-coefficient equations in (1+1) dimensions. Let us consider the following two variable-coefficient (1+1)-dimensional nonlinear equations:

$$G_y + \left(\frac{yt}{2\sigma^2} - \frac{\alpha_1 t}{\sigma}\right)G_x - \frac{2\sqrt{3}\epsilon t}{\sigma}GG_x - \frac{2\sqrt{3}\epsilon t}{\sigma}H_x + \frac{\sqrt{3}\epsilon t}{\sigma}G_{xx} = 0, \tag{4}$$

$$H_y + \left(\frac{yt}{2\sigma^2} - \frac{\alpha_1 t}{\sigma}\right)H_x - \frac{2\sqrt{3}\epsilon t}{\sigma}(GH)_x - \frac{\sqrt{3}\epsilon t}{\sigma}H_{xx} = 0 \tag{5}$$

and

$$\begin{aligned} G_t - \frac{\sqrt{3}\epsilon y}{\sigma}(2GG_x + 2H_x - G_{xx}) + 4(6GH - 3GG_x + G^3)_x \\ + \left(\frac{y^2}{4\sigma^2} - \frac{\alpha_1 y}{\sigma} + \alpha_1^2\right)G_x + 2\sqrt{3}\epsilon\alpha_1(G^2 + 2H - G_x)_x + 4G_{xxx} = 0, \end{aligned} \tag{6}$$

$$\begin{aligned} H_t - 2\sqrt{3}\epsilon\left(\frac{y}{\sigma} - 2\alpha_1\right)(GH)_x + 12(G^2H + H^2 + GH_x)_x \\ + \left(\frac{y^2}{4\sigma^2} - \frac{y\alpha_1}{\sigma} + \alpha_1^2\right)H_x - \sqrt{3}\epsilon\left(\frac{y}{\sigma} - 2\alpha_1\right)H_{xx} + 4H_{xxx} = 0, \end{aligned} \tag{7}$$

where $\epsilon = \pm 1$ and α_1 is an arbitrary constant.

We regard (G, H) as a compatible solution of equations (4)–(7) and make the transformation [26]

$$u = 2H. \tag{8}$$

Making use of equations (4)–(7), one can get

$$\begin{aligned} G_y &= -\left(\frac{yt}{2\sigma^2} - \frac{\alpha_1 t}{\sigma}\right)G_x + \frac{2\sqrt{3}\epsilon t}{\sigma}GG_x + \frac{\sqrt{3}\epsilon t}{\sigma}u_x - \frac{\sqrt{3}\epsilon t}{\sigma}G_{xx}, \\ u_y &= -\left(\frac{yt}{2\sigma^2} - \frac{\alpha_1 t}{\sigma}\right)u_x + \frac{2\sqrt{3}\epsilon t}{\sigma}(Gu)_x + \frac{\sqrt{3}\epsilon t}{\sigma}u_{xx}, \\ u_t &= 2\sqrt{3}\epsilon\left(\frac{y}{\sigma} - 2\alpha_1\right)(Gu)_x - 12\left(G^2u + \frac{1}{2}u^2 + Gu_x\right)_x \\ &\quad - \left(\frac{y^2}{4\sigma^2} - \frac{y\alpha_1}{\sigma} + \alpha_1^2\right)u_x + \sqrt{3}\epsilon\left(\frac{y}{\sigma} - 2\alpha_1\right)u_{xx} - 4u_{xxx}. \end{aligned}$$

With symbolic computation, we can prove that u satisfies equation (2). Therefore, it is clear that if (G, H) is a compatible solution of equations (4)–(7), then u determined by expression (8) is a solution of equation (2).

3. Construction of DTs for equations (4)–(7) with symbolic computation

In this section, we will symbolically construct three kinds of DTs for equations (4)–(7). Equations (4) and (5) have the following Lax representation:

$$\Phi_x = U\Phi, \qquad U = \begin{pmatrix} \frac{1}{2}(-\lambda - G) & -H \\ 1 & \frac{1}{2}(\lambda + G) \end{pmatrix}, \tag{9}$$

$$\Phi_y = V\Phi, \qquad V = \begin{pmatrix} V_{11} & V_{12} \\ V_{21} & -V_{11} \end{pmatrix}, \tag{10}$$

with

$$V_{11} = \frac{\sqrt{3}\epsilon t}{2\sigma}\left(\lambda^2 - G^2 - G_x - \frac{2GH_x}{H} - \frac{H_{xx}}{H}\right) + \left(\frac{yt}{4\sigma^2} - \frac{\alpha_1 t}{2\sigma}\right)\left(\lambda + G + \frac{H_x}{H}\right) + \frac{H_y}{2H},$$

$$V_{12} = \frac{\sqrt{3}\epsilon t}{\sigma}(H\lambda - H_x - GH) + \left(\frac{yt}{2\sigma^2} - \frac{\alpha_1 t}{\sigma}\right)H,$$

$$V_{21} = \frac{\sqrt{3}\epsilon t}{\sigma}(-\lambda + G) + \frac{\alpha_1 t}{\sigma} - \frac{yt}{2\sigma^2},$$

where λ is the isospectral parameter. From the compatibility condition $U_y - V_x + UV - VU = 0$, one can derive equations (4) and (5).

In addition, the Lax representation of equations (6) and (7) is the spectral problem (9) and the auxiliary problem

$$\Phi_t = W\Phi, \qquad W = \begin{pmatrix} W_{11} & W_{12} \\ W_{21} & -W_{11} \end{pmatrix}, \tag{11}$$

with

$$\begin{aligned} W_{11} = {} & 2\lambda^3 - \frac{\sqrt{3}\epsilon}{2\sigma}(y - 2\sigma\alpha_1)\left(-\lambda^2 + G^2 + G_x + 2\frac{GH_x}{H} + \frac{H_{xx}}{H}\right) \\ & + \frac{1}{8\sigma^2}(y - 2\sigma\alpha_1)^2\lambda + 4\lambda H + \frac{1}{2}\left(\frac{y^2}{4\sigma^2} - \frac{\alpha_1 y}{\sigma} + \alpha_1^2\right)\left(G + \frac{H_x}{H}\right) \\ & + \frac{1}{2H}[H_t + 12(GH_x)_x + 12G^2H_x + 4H_{xxx}] \\ & + 2G_{xx} + 6GG_x + 8H_x + 2G^3 + 4GH, \end{aligned}$$

$$\begin{aligned} W_{12} = {} & 4\lambda^2 H - \lambda\left(4H_x + 4GH + 2\sqrt{3}\epsilon\alpha_1 H - \frac{\sqrt{3}\epsilon y}{\sigma}H\right) - \frac{\sqrt{3}\epsilon}{\sigma}(y - 2\sigma\alpha_1)(GH + H_x) \\ & + \left(\frac{y^2}{4\sigma^2} - \frac{\alpha_1 y}{\sigma} + \alpha_1^2\right)H + 4H_{xx} + 4HG_x + 8GH_x + 8H^2 + 4G^2H, \end{aligned}$$

$$\begin{aligned} W_{21} = {} & -4\lambda^2 + \lambda\left(4G + 2\sqrt{3}\epsilon\alpha_1 - \frac{\sqrt{3}\epsilon y}{\sigma}\right) + 4G_x - 4G^2 \\ & + \frac{\sqrt{3}\epsilon}{\sigma}(y - 2\sigma\alpha_1)G - 8H - \frac{y^2}{4\sigma^2} + \frac{\alpha_1 y}{\sigma} - \alpha_1^2. \end{aligned}$$

By virtue of symbolic computation, equations (6) and (7) can be recovered by the compatibility condition $U_t - W_x + UW - WU = 0$.

It is well known that the DT is an important and effective tool to generate the multi-soliton solutions of integrable NLEEs. For the Lax representation (9)–(11), we can actually construct three kinds of DTs including two basic DTs and a complex DT, as shown in [32]. In the following, we assume that the DT has the form

$$\hat{\Phi} = T\Phi. \tag{12}$$

In order to make $\hat{\Phi}$ satisfy

$$\hat{\Phi}_x = \hat{U}\hat{\Phi}, \qquad \hat{\Phi}_y = \hat{V}\hat{\Phi}, \qquad \hat{\Phi}_t = \hat{W}\hat{\Phi}, \tag{13}$$

where $\hat{U}$, $\hat{V}$ and $\hat{W}$ are the same as U, V and W except that G, H, G_x, H_x, H_{xx}, H_{xxx}, H_y and H_t are respectively replaced with $\hat{G}$, $\hat{H}$, $\hat{G}_x$, $\hat{H}_x$, $\hat{H}_{xx}$, $\hat{H}_{xxx}$, $\hat{H}_y$ and $\hat{H}_t$, T must satisfy the following relations:

$$T_x + TU - \hat{U}T = 0, \tag{14}$$

$$T_y + TV - \hat{V}T = 0, \tag{15}$$

$$T_t + TW - \hat{W}T = 0. \tag{16}$$

3.1. First DT

Suppose that

$$T_1 = \delta_1 \begin{pmatrix} \lambda + a_1 & b_1 \\ c_1 & d_1 \end{pmatrix}, \tag{17}$$

where δ_1, a_1, b_1, c_1 and d_1 are all analytic functions of x, y and t to be determined.

Substituting transformation (17) into equation (14) with symbolic computation and equating the coefficient matrices of the terms λ^i $(i = 0, 1, 2)$ to be zero, we obtain

$$\hat{G} = G - 2\frac{\delta_{1,x}}{\delta_1}, \qquad c_1 = -1, \qquad b_1 = H, \tag{18}$$

$$\hat{H} = H + a_{1,x}, \tag{19}$$

$$GH - H\delta_1 + \hat{H}d_1 = 0, \tag{20}$$

$$G - a_1 + d_1 - 2\frac{\delta_{1,x}}{\delta_1} = 0, \tag{21}$$

$$\delta_1 = \beta_1 \frac{1}{\sqrt{d_1}}, \tag{22}$$

where β_1 is an arbitrary constant. Combining equations (18) and (21) yields

$$\hat{G} = a_1 - d_1. \tag{23}$$

On the other hand, let $(\varphi_1(\lambda_1), \varphi_2(\lambda_1))^*$, where the prime * denotes the transpose of the matrix, be a solution of the Lax representation (9)–(11) with $\lambda = \lambda_1$, then we have

$$(\lambda_1 + a_1)\varphi_1(\lambda_1) + b_1\varphi_2(\lambda_1) = 0,$$
$$c_1\varphi_1(\lambda_1) + d_1\varphi_2(\lambda_1) = 0,$$

which give rise to

$$a_1 = -\lambda_1 - H\frac{\varphi_2(\lambda_1)}{\varphi_1(\lambda_1)}, \qquad d_1 = \frac{\varphi_1(\lambda_1)}{\varphi_2(\lambda_1)},$$

so $\hat{G}$ and $\hat{H}$ can be rewritten as

$$\hat{G} = -\lambda_1 - H\frac{\varphi_2(\lambda_1)}{\varphi_1(\lambda_1)} - \frac{\varphi_1(\lambda_1)}{\varphi_2(\lambda_1)}, \qquad \hat{H} = H - \left[H\frac{\varphi_2(\lambda_1)}{\varphi_1(\lambda_1)}\right]_x. \tag{24}$$

With the aid of symbolic computation, it can be proved that equations (20) and (21) are satisfied automatically.

The key for constructing DT is to make the Lax representation (9)–(11) invariant under transformation (17). In order to assure transformation (17) is a DT in theory, one has to verify that it also satisfies equations (15) and (16). The above demonstration is rather intricate since expressions (10) and (11) are comparatively complicated in the format. Hence, we will use *Mathematica* to handle the calculation.

Substituting transformation (17) with the expressions V, W, $\hat{V}$ and $\hat{W}$ into expressions (10) and (11), we assume that the resulting expressions are of the form

$$T_y + TV - \hat{V}T = \begin{pmatrix} M_{11} & M_{12} \\ M_{21} & M_{22} \end{pmatrix}, \tag{25}$$

$$T_t + TW - \hat{W}T = \begin{pmatrix} N_{11} & N_{12} \\ N_{21} & N_{22} \end{pmatrix}. \tag{26}$$

It is shown that the entries M_{ij} and N_{ij} $(i, j = 1, 2)$ are too long and tedious to present in the paper. However, by virtue of symbolic computation, it is easy to verify that these expressions with the substitution of $\varphi_{i,xxxx}(\lambda_1)$, $\varphi_{i,xxx}(\lambda_1)$, $\varphi_{i,xx}(\lambda_1)$, $\varphi_{i,xy}(\lambda_1)$, $\varphi_{i,xt}(\lambda_1)$, $\varphi_{i,x}(\lambda_1)$, $\varphi_{i,y}(\lambda_1)$, $\varphi_{i,t}(\lambda_1)$, H_{xy}, H_{xt}, H_y, H_t, G_y and G_t $(i = 1, 2)$ are satisfied automatically. Therefore, we obtain the explicit expression of the first DT.

3.2. Second DT

Analogous to the process in subsection 3.1, it is easy to show that the second DT is of the form

$$T_2 = \delta_2 \begin{pmatrix} a_2 & b_2 \\ c_2 & \lambda + d_2 \end{pmatrix}, \tag{27}$$

with

$$\begin{aligned} &a_2 = -b_2\frac{\varphi_2(\lambda_2)}{\varphi_1(\lambda_2)}, \qquad b_2 = -H + d_{2,x}, \qquad c_2 = 1, \qquad d_2 = -\lambda_2 - \frac{\varphi_1(\lambda_2)}{\varphi_2(\lambda_2)}, \\ &\delta_2 = \beta_2\frac{1}{\sqrt{a_2}}, \qquad \hat{G} = G - \frac{a_{2,x}}{a_2}, \qquad \hat{H} = H - d_{2,x}, \end{aligned} \tag{28}$$

where β_2 is an arbitrary constant and $(\varphi_1(\lambda_2), \varphi_2(\lambda_2))^*$ is a solution of the Lax representation (9)–(11) with $\lambda = \lambda_2$.

3.3. Third DT

By proceeding as before, the third DT can be expressed as

$$T_3 = \begin{pmatrix} \delta_3(\lambda + a_3) & \delta_3 b_3 \\ \theta_3 c_3 & \theta_3(\lambda + d_3) \end{pmatrix}, \tag{29}$$

with

$$a_3 = -\frac{\lambda_4\varphi_2(\lambda_3)\varphi_1(\lambda_4) - \lambda_3\varphi_1(\lambda_3)\varphi_2(\lambda_4)}{\Delta},$$

$$b_3 = \frac{(\lambda_4 - \lambda_3)\varphi_1(\lambda_3)\varphi_1(\lambda_4)}{\Delta},$$

$$
\begin{aligned}
c_3 &= \frac{(\lambda_3-\lambda_4)\varphi_2(\lambda_3)\varphi_2(\lambda_4)}{\Delta},\\
d_3 &= \frac{\lambda_4\varphi_1(\lambda_3)\varphi_2(\lambda_4)-\lambda_3\varphi_2(\lambda_3)\varphi_1(\lambda_4)}{\Delta},\\
\delta_3 &= \sqrt{1-c_3}, \qquad \theta_3 = \frac{\beta_3}{\sqrt{1-c_3}},\\
\hat{G} &= G - \frac{\partial}{\partial x}\log(1-c_3), \qquad \hat{H} = (1-c_3)(H-b_3),
\end{aligned}
\tag{30}
$$

where $\Delta = \varphi_2(\lambda_3)\varphi_1(\lambda_4) - \varphi_1(\lambda_3)\varphi_2(\lambda_4)$ and β_3 is an arbitrary constant, while $(\varphi_1(\lambda_3), \varphi_2(\lambda_3))^*$ and $(\varphi_1(\lambda_4), \varphi_2(\lambda_4))^*$ are two solutions of the Lax representation (9)–(11) with $\lambda = \lambda_3$ and $\lambda = \lambda_4$, respectively.

Considering the similar calculation, we can prove that transformations (27) and (29) are also indeed DTs. According to the above testifications, these three DTs obtained in this paper can transform the Lax representation (9)–(11) into the equivalent linear system, i.e., $\hat{\Phi}_x = \hat{U}\hat{\Phi}$, $\hat{\Phi}_y = \hat{V}\hat{\Phi}$ and $\hat{\Phi}_t = \hat{W}\hat{\Phi}$. Consequently, the two Lax representations can give rise to the same equations (4)–(7) and these three kinds of functions $(\hat{G}, \hat{H})$ defined in subsections 3.1, 3.2 and 3.3 are three new solutions of equations (4)–(7). From what have been investigated in sections 2 and 3, we can draw the following conclusion.

Let (G, H) be a compatible solution of equations (4)–(7), then $(\hat{G}, \hat{H})$ defined respectively by equations (24), (28) and (30) are three types of solutions of equations (4)–(7). Thus,

$$\hat{u} = 2\hat{H} \tag{31}$$

corresponds to a new solution of the cylindrical KP equation, i.e., equation (2).

In fact, one can prove that $T_1(\lambda_1)T_2(\lambda_2) = T_3(\lambda_1, \lambda_2)$ by symbolic computation (detail ignored) as in [33]. In other words, if we do the first basic DT to map (G, H) to $(\hat{G}, \hat{H})$ and then carry out the second basic DT to transform $(\hat{G}, \hat{H})$ to (G_2, H_2), then we can see that (G_2, H_2) is identical with the result through performing the third DT only once.

4. Multi-soliton-like solutions

In this section, the multi-soliton-like solutions of equation (1) will be explicitly constructed by these three DTs: (17), (27) and (29). We take $G = 0$ and $H = 1$ as our 'seed' solution since it is a trivial solution of equations (4)–(7) and $u = 2H = 1$ is also a paltry solution of equation (2). Substituting $G = 0$ and $H = 1$ into the Lax representation (9)–(11) yields the solutions with $\lambda = \lambda_j$ $(j = 1, 2, 3, \ldots)$ as

$$
\begin{aligned}
\varphi_1(\lambda_j) &= \mathrm{e}^{\kappa_j\zeta_j} + \mathrm{e}^{-\kappa_j\zeta_j},\\
\varphi_2(\lambda_j) &= \left(-\kappa_j - \frac{\lambda_j}{2}\right)\mathrm{e}^{\kappa_j\zeta_j} + \left(\kappa_j - \frac{\lambda_j}{2}\right)\mathrm{e}^{-\kappa_j\zeta_j},
\end{aligned}
$$

where

$$\kappa_j = \sqrt{\frac{\lambda_j^2}{4} - 1}, \tag{32}$$

$$\zeta_j = x - t\left[\left(4\lambda_j^2 - 2\sqrt{3}\epsilon\alpha_1\lambda_j + \alpha_1^2 + 8\right) + \frac{\left(y^2 + 4\sqrt{3}\sigma\epsilon\lambda_j y - 4\sigma\alpha_1 y\right)}{4\sigma^2}\right]. \tag{33}$$

4.1. One-soliton-like solutions of equation (1)

For the first DT, using equations (8) and (24) leads to a new solution of equation (2)

$$u_1[1] = 2\hat{H} = 2\left[1 + \kappa_1^2 \operatorname{sech}^2(\kappa_1\zeta_1)\right], \tag{34}$$

with κ_1 and ζ_1 as defined above. Similarly, for the second DT, another new solution of equation (2) can be obtained from equations (8) and (28)

$$u_2[1] = 2\hat{H} = 2\left[1 + \frac{4\kappa_2^2 \operatorname{sech}^2(\kappa_2\zeta_2)}{\lambda_2 + 2\kappa_2 \tanh^2(\kappa_2\zeta_2)}\right], \tag{35}$$

where κ_2 and ζ_2 have been defined in expressions (32) and (33).

Furthermore, through the scaling transformation (3), we can obtain two types of soliton-like solutions of equation (1) as

$$\phi_1[1] = -\frac{12D}{A}\left[1 + \kappa_1^2 \operatorname{sech}^2(\kappa_1\vartheta_1)\right], \tag{36}$$

$$\phi_2[1] = -\frac{12D}{A}\left[1 + \frac{4\kappa_2^2 \operatorname{sech}^2(\kappa_2\vartheta_2)}{\lambda_2 + 2\kappa_2 \tanh^2(\kappa_2\vartheta_2)}\right], \tag{37}$$

where $\vartheta_i = \xi - D\tau\left[\left(4\lambda_j^2 - 2\sqrt{3}\epsilon\alpha_1\lambda_j + \alpha_1^2 + 8\right) + \eta\left(c\eta + 2\sqrt{6cD}\epsilon\lambda_j - 2\sqrt{2cD}\alpha_1\right)/2D\right]$ $(i = 1, 2)$.

Both expressions (36) and (37) possess soliton-like structures, which might be very useful for the description of some physical phenomena such as the evolution of the ring dark soliton in a Bose–Einstein condensate with a thin disc-shaped potential [1], the dust-acoustic wave propagation in a cosmic dusty plasma [2] and the relativistically magnetosonic solitary wave propagating in a collisionless plasma [6]. For convenience, we only discuss expression (36) and neglect expression (37) since the latter has the similar properties to the former.

It is shown in expression (36) that the amplitude of the solitary wave is merely dependent on the physical parameter of the dusty plasma such as μ_l, μ_h, β_1 and β_2. For the dusty plasma with two-temperature ions, the dust-acoustic soliton-like structures are rarefactive if $A/D > 0$, while compressive with $A/D < 0$ [5]. As claimed in [5], if the rarefactive solitary-wave/soliton-like structures exist, the phase velocity should satisfy $c^2 > F$, where $F = \left(\gamma_d B^2 - 2B^2 + \beta_1^2 - \beta_1^2\mu_h + \beta_2^2\mu_h - \beta_1^2\mu_l + \mu_l\right)/B^3 s\,(\gamma_d + 1)$. Whereas, if the solitary-wave/soliton-like structures are compressive, the condition for the phase velocity to be satisfied is $0 < c^2 < F$. Then, the temperatures of ions and electrons will significantly affect the existence and amplitude of the compressive and rarefactive soliton structures [5].

In order to better understand the mechanism of the propagation of dust-acoustic solitary waves with the development of time, we will draw some pictures via expression (36) in line with the dusty plasma background.

Figure 1 displays the compressive parabola-soliton-like profile, where the choice of the physical parameters in the dusty plasma with two-temperature ions is based on the available data presented in [5]. Furthermore, it is worth noting that the transverse perturbation (η) significantly affects the soliton structure (see figure 1). When the transverse perturbation (η) is small, we know that the shape of the soliton keeps unchangeable during the propagation process of the soliton as shown in figure 1(*a*), which is identical with the result in [5]. However, if the transverse perturbation (η) becomes larger, the soliton warps in certain radian with invariant amplitude (see figures 1(*b*)–(*f*)). Additionally, the solitary wave solution is a parabola soliton and its shape will slightly deform with the time going on. As seen in figures 1(*b*)–(*f*), the structure of the parabola soliton is 'out-going' and opens horizontally to the negative ξ-axis with $-\infty < \tau < 0$, while it is 'in-going' and opens to the positive ξ-axis

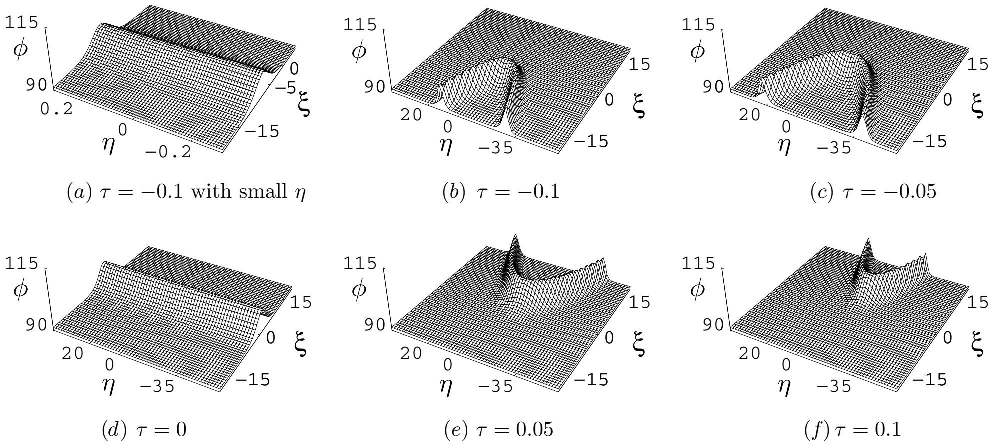

(*a*) $\tau = -0.1$ with small η (*b*) $\tau = -0.1$ (*c*) $\tau = -0.05$

(*d*) $\tau = 0$ (*e*) $\tau = 0.05$ (*f*) $\tau = 0.1$

Figure 1. The same parameters for (*a*)–(*f*) are $\gamma_d = 3, c = \sqrt{0.5}, \mu_l = \mu_h = 0.6, \beta_1 = 1, \beta_2 = 0.01, s = 0.5, \alpha_1 = \epsilon = 1$ and $\lambda_1 = 2.1$. (*a*) The one-compressive soliton structure for expression (36) with small η at $\tau = -0.1$. (*b*)–(*f*) The one-parabola-soliton solution surfaces via expression (36) with large η and different values of τ.

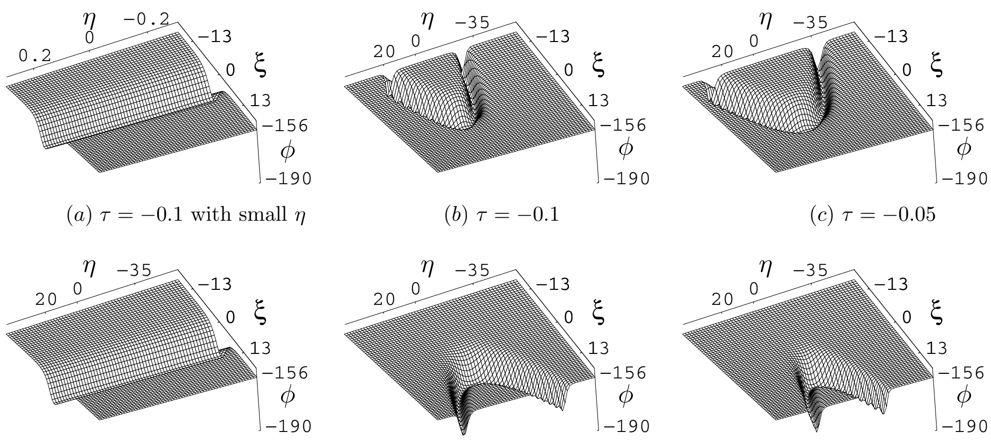

(*a*) $\tau = -0.1$ with small η (*b*) $\tau = -0.1$ (*c*) $\tau = -0.05$

(*d*) $\tau = 0$ (*e*) $\tau = 0.05$ (*f*) $\tau = 0.1$

Figure 2. The one-rarefactive-parabola soliton surfaces for expression (36) with the same physical parameters as in figure (1) except for $\mu_h = 1$. (*a*) The one-soliton-like solution surface via expression (36) with small η at $\tau = -0.1$. (*b*)–(*f*) The one-soliton-like solution surfaces via expression (36) with large η and different values of τ.

with $0 < \tau < \infty$. When $\tau = 0$, it reduces to a static soliton as illustrated in figure 1(*d*). The vertex of the parabola soliton is variable along the axis of symmetry as time goes on.

In fact, for suitable choice of the values of the physical parameters in the dusty plasma with two-temperature ions, we can get the rarefactive parabola soliton (see figure 2). We also note that figure 2 has the similar properties as those in figure 1.

Figures 1 and 2 show that the parabola soliton forms a part of a loop soliton. As stated in [34], several transition region and coronal explorer (TRACE) images have indicated the observation of this morphology in the coronal plasma, i.e., the long-duration post-flare

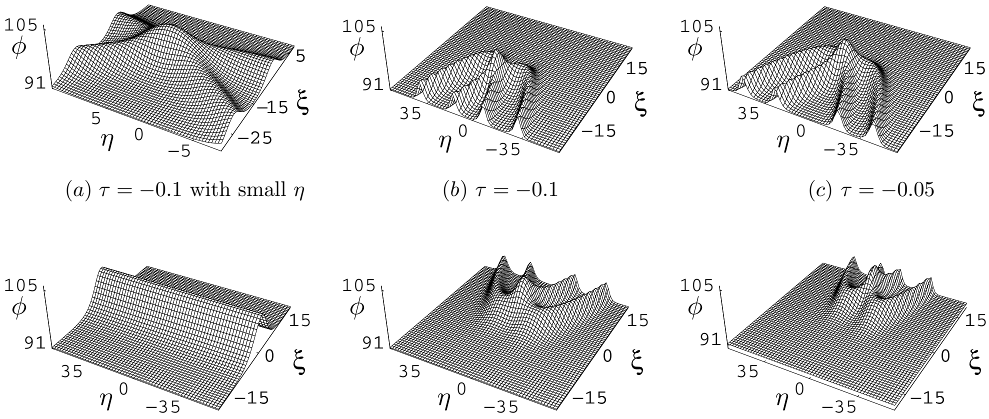

(a) $\tau = -0.1$ with small η (b) $\tau = -0.1$ (c) $\tau = -0.05$

(d) $\tau = 0$ (e) $\tau = 0.05$ (f) $\tau = 0.1$

Figure 3. The same parameters for (a)–(f) are $\gamma_d = 3, c = \sqrt{0.5}, \mu_l = \mu_h = 0.6, \beta_1 = 1, \beta_2 = 0.01, s = 0.5, \alpha_1 = \epsilon = 1, \lambda_1 = 2.05$ and $\lambda_2 = -2.05$. (a) The compressive soliton structure via expression (38) with small η at $\tau = -0.1$. (b)–(f) The two-parabola-soliton solution surfaces for expression (38) with large η and different values of τ.

loops [5]. We also hope that such morphology may be helpful for investigating the dust-acoustic wave propagation in the dusty plasma [1, 5] and in a cosmic dusty plasma environment such as the supernova shells or Saturn's F-ring [2, 22].

4.2. Two-soliton-like solution of equation (1)

Utilizing the third DT (29) and equations (30) gives the new solution $(\hat{G}_3[2], \hat{H}_3[2])$ of equations (4)–(7). Therefore, the two-soliton-like solution of equation (1) is of the form

$$\phi_3[2] = -\frac{12D}{A}\left[1 - \frac{2(\lambda_3 - \lambda_4)}{X_3 - X_4}\right]\left[1 + \frac{(\lambda_3 - \lambda_4)X_3X_4}{2\,(X_3 - X_4)}\right], \tag{38}$$

where $\lambda_3 \neq \lambda_4, X_3 = \lambda_3 + 2\kappa_3 \tanh(\kappa_3\vartheta_3)$ and $X_4 = \lambda_4 + 2\kappa_4 \tanh(\kappa_4\vartheta_4)$, with κ_j and ϑ_j $(j = 3, 4)$ as defined in subsection 4.1.

Expression (38) can also present two types of dust-acoustic wave structures, namely, the compressive and rarefactive solitons, when the physical parameters involved in the system are chosen suitably. To illustrate the above two structures, we plot some pictures at different values of τ on the basis of the data in [5] (see figures 3 and 4).

With different values for the physical parameters included in expression (38), figures 3 and 4 display the compressive and rarefactive soliton interaction structures, respectively. Additionally, from the above two sets of photographs, we can also see the significant influence of the transverse perturbation (η) on the soliton structure. It is shown in figures 3 and 4 that there is no change of shapes between solitons after the interaction except for a phase shift. Thus, it can be concluded that expression (38) has the following characteristics: (i) its soliton structure is 'out-going' and opens horizontally to the minus side of the ξ-axis with $-\infty < \tau < 0$, while it is 'in-going' and opens to the plus side of the ξ-axis with $0 < \tau < \infty$; (ii) when $\tau = 0$, it degenerates into a static single soliton (see figures 3(d) and 4(d)); (iii) the vertex of each parabola soliton is variable along the corresponding axis of symmetry as the time goes on.

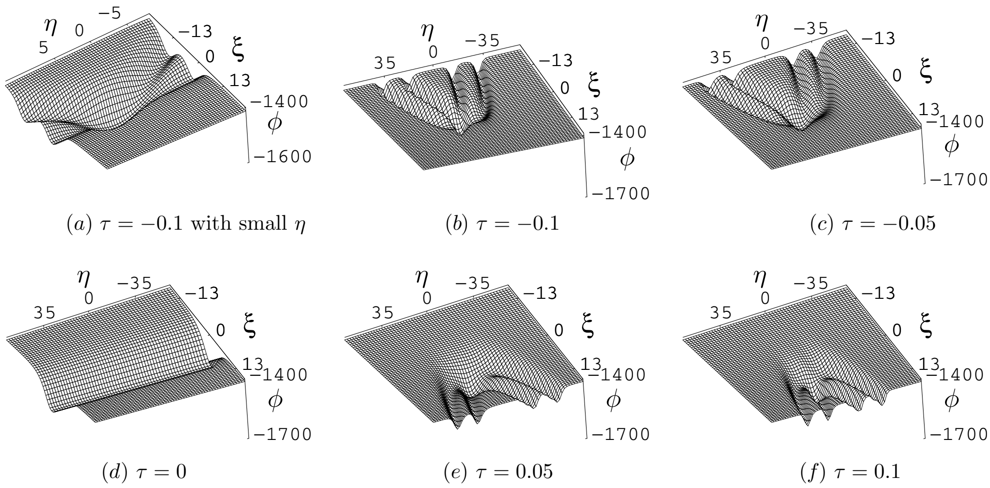

(a) $\tau = -0.1$ with small η (b) $\tau = -0.1$ (c) $\tau = -0.05$

(d) $\tau = 0$ (e) $\tau = 0.05$ (f) $\tau = 0.1$

Figure 4. The two-rarefactive soliton structure for expression (38) with the same physical parameters as in figure 3 except for $\mu_h = 0.9$. (a) The two-soliton-like solution surface via expression (38) with small η at $\tau = -0.1$. (b)–(f) The two-parabola-soliton solution surfaces via expression (38) with large η and different values of τ.

Though equation (1) in the non-planar cylindrical geometry is obviously different from the planar-geometry KP equation in [11], the former is transformable to the latter because of the existence of a Lie-point transformation [23]. Thus, analogous results to those in [11] for the KP equation in planar geometry can be obtained for equation (1) such as the *N*-soliton solution, cnoidal wave-typed solution, an infinite series of conservation laws and stability of the solitary waves. However, it should be noted that the one- and two-soliton-like solutions obtained in this section are distinct from the results in [11] due to the difference of geometry [17].

4.3. Three-soliton-like solution of equation (1)

We choose $\lambda_5 \neq \lambda_4 \neq \lambda_3$ and transform $(\hat{G}_3[2], \hat{H}_3[2])$ to $(\hat{G}_{3,1}[3], \hat{H}_{3,1}[3])$ using the first basic DT (17). Assuming

$$\Theta(x, y, t) = \frac{\beta_3[c_3\varphi_1(\lambda_5) + (\lambda_5 + d_3)\varphi_2(\lambda_5)]}{(1 - c_3)[(\lambda_5 + a_3)\varphi_1(\lambda_5) + b_3\varphi_2(\lambda_5)]} \tag{39}$$

and using equation (24) yield

$$\hat{G}_{3,1}[3] = -\lambda_5 - \frac{\hat{H}_3[2]\Theta^2 + 1}{\Theta}, \tag{40}$$

$$\hat{H}_{3,1}[3] = \hat{H}_3[2] - (\hat{H}_3[2]\Theta)_x. \tag{41}$$

Correspondingly, we can get the three-soliton-like solution of equation (2) as

$$u_{3,1}[3] = 2\hat{H}_{3,1}[3] = 2[\hat{H}_3[2] - (\hat{H}_3[2]\Theta)_x]. \tag{42}$$

By the scaling transformation (3) and expression (42), the three-soliton-like solution of equation (1) can also be expressed explicitly.

4.4. Four-soliton-like solution of equation (1)

We take $\lambda_6 \neq \lambda_5 \neq \lambda_4 \neq \lambda_3$ and iterate the third DT (29) once again to convert $(\hat{G}_3[2], \hat{H}_3[2])$ to $(\hat{G}_3[4], \hat{H}_3[4])$.

By setting

$$\begin{aligned}
&\hat{\Omega}_1(\lambda_5) = \delta_3[(\lambda_5 + a_3)\varphi_1(\lambda_5) + b_3\varphi_2(\lambda_5)] = \delta_3\Psi_1(\lambda_5),\\
&\hat{\Omega}_2(\lambda_5) = \theta_3[c_3\varphi_1(\lambda_5) + (\lambda_5 + d_3)\varphi_2(\lambda_5)] = \theta_3\Psi_2(\lambda_5),\\
&\hat{\Omega}_1(\lambda_6) = \delta_3[(\lambda_6 + a_3)\varphi_1(\lambda_6) + b_3\varphi_2(\lambda_6)] = \delta_3\Psi_1(\lambda_6),\\
&\hat{\Omega}_2(\lambda_6) = \theta_3[c_3\varphi_1(\lambda_6) + (\lambda_6 + d_3)\varphi_2(\lambda_6)] = \theta_3\Psi_2(\lambda_6),\\
&\hat{\Delta} = \Psi_2(\lambda_5)\Psi_1(\lambda_6) - \Psi_1(\lambda_5)\Psi_2(\lambda_6),\\
&\hat{a}_3 = -\frac{\lambda_6\Psi_2(\lambda_5)\Psi_1(\lambda_6) - \lambda_5\Psi_1(\lambda_5)\Psi_2(\lambda_6)}{\hat{\Delta}},\\
&\hat{b}_3 = \frac{(1-c_3)(\lambda_6-\lambda_5)\Psi_1(\lambda_5)\Psi_1(\lambda_6)}{\beta_3\hat{\Delta}},\\
&\hat{c}_3 = \frac{\beta_3(\lambda_5-\lambda_6)\Psi_2(\lambda_5)\Psi_2(\lambda_6)}{(1-c_3)\hat{\Delta}},\\
&\hat{d}_3 = \frac{\lambda_6\Psi_1(\lambda_5)\Psi_2(\lambda_6) - \lambda_5\Psi_2(\lambda_5)\Psi_1(\lambda_6)}{\hat{\Delta}},
\end{aligned}$$

we have

$$\begin{aligned}
&\hat{G}_3[4] = \hat{G}_3[2] - \frac{\partial}{\partial x}\log(1-\hat{c}_3),\\
&\hat{H}_3[4] = (1-\hat{c}_3)(\hat{H}_3[2] - \hat{b}_3),
\end{aligned}$$

which is a compatible solution of equations (4)–(7), and get the four-soliton-like solution of equation (2),

$$u_3[4] = 2\hat{H}_3[4] = 2(1-\hat{c}_3)(\hat{H}_3[2] - \hat{b}_3). \tag{43}$$

Similarly, we can obtain the four-soliton-like solution of equation (1) through the scaling transformation (3) and expression (43).

5. Conclusions

In this paper, the cylindrical KP equation, i.e., equation (1), is under investigation which can describe the propagation of dust-acoustic waves in the dusty plasma consisting of cold dust particles, an unmagnified, collisionless, isothermal electron and two-temperature ions. Through the decomposition method, such a (2+1)-dimensional equation has been decomposed into two variable-coefficient (1+1)-dimensional integrable NLEEs of the same hierarchy. Three kinds of DTs for these two (1+1)-dimensional equations have been constructed and the multi-soliton-like solutions of equation (1) have also been explicitly obtained. Of physical interest, we have specially analysed the one- and two-parabola-soliton solutions for equation (1). Through the graphical analysis for some sample solutions, we have discussed the effects resulting from the physical parameters in the dusty plasma and transverse perturbation, and pointed out some possible applications in the Bose–Einstein condensates, the dusty plasma with two-temperature ions and a cosmic dusty plasma environment such as the supernova shells or Saturn's F-ring.

Acknowledgments

We express our thanks to the referees and Professor Y T Gao for their valuable comments. This work has been supported by the Key Project of Chinese Ministry of Education (no 106033), by the Specialized Research Fund for the Doctoral Program of Higher Education (no 20060006024), Chinese Ministry of Education and by the National Natural Science Foundation of China under grant no 60372095.

References

[1] Xue J K 2004 *J. Phys. A: Math. Gen.* **37** 11223
[2] Hong W P 2007 *Phys. Lett.* A **361** 520
Tian B and Gao Y T 2005 *Phys. Plasmas (Lett.)* **12** 070703
Tian B and Gao Y T 2005 *Phys. Lett.* A **340** 243
Tian B and Gao Y T 2005 *Phys. Lett.* A **340** 449
Gao Y T and Tian B 2006 *Phys. Plasmas (Lett.)* **13** 120703
Gao Y T and Tian B 2007 *Phys. Lett.* A **361** 523
Gao Y T and Tian B 2007 *Europhys. Lett.* **77** 15001
[3] Tian B and Gao Y T 2005 *Eur. Phys. J.* D **33** 59
[4] Franz J R, Kintner P M and Pickett J S 1998 *Geophys. Res. Lett.* **25** 2041
[5] Gao Y T and Tian B 2006 *Phys. Lett.* A **349** 314
Wang Y Y and Zhang J F 2006 *Phys. Lett.* A **352** 155
[6] Wang Y L, Zhou Z X, Jiang X Q, Zhang H F, Jiang Y Y, Hou C F, Sun X D and Qin R H 2006 *Phys. Lett.* A **355** 386
[7] Kadomtsev B B and Petviashvili V I 1970 *Sov. Phys.—Dokl.* **15** 539
[8] Santini P M 1981 *Lett. Nuovo Cimento* **30** 236
[9] David D, Levi D and Winternitz P 1987 *Stud. Appl. Math.* **76** 133
David D, Levi D and Winternitz P 1989 *Stud. Appl. Math.* **80** 1
[10] Duan W S 2002 *Chaos Solitons Fractals* **14** 1315
Lin M M and Duan W S 2005 *Chaos Solitons Fractals* **23** 929
[11] Belashov V Y and Vladimirov S V 2005 *Solitary Waves in Dispersive Complex Media* (Berlin: Springer)
[12] Moslem W M 2005 *Chaos Solitons Fractals* **23** 939
Zhang J F and Wang Y Y 2006 *Phys. Plasmas* **13** 022303
[13] Tagare S G 1997 *Phys. Plasmas* **4** 3167
[14] Xie B S, He K F and Huang Z Q 1999 *Phys. Plasmas* **6** 3808
[15] Barkan A, Angelo N D and Merlino R L 1994 *Phys. Rev. Lett.* **73** 3093
[16] Gill T S, Saini N S and Kaur H 2006 *Chaos Solitons Fractals* **28** 1106
[17] Xue J K 2005 *Phys. Plasmas* **12** 012314
[18] Vladimirov S V, Ostrikov K and Samarian A A 2005 *Physics and Applications of Complex Plasmas* (London: Imperial College Press)
[19] Ostrikov K N, Vladimirov S V, Yu M Y and Morfill G E 2000 *Phys. Rev.* E **61** 4315
[20] Vladimirov S V, Ostrikov K N, Yu M Y and Morfill G E 2003 *Phys. Rev.* E **67** 036406
Tsytovich V N, Vladimirov S V and Morfill G E 2004 *Phys. Rev.* E **70** 066408
[21] Vladimirov S V and Ostrikov K 2004 *Phys. Rep.* **393** 175
[22] Mendis D A 2002 *Plasmas Sources Sci. Technol.* A **11** 219
[23] Clarkson P A 1990 *IMA J. Appl. Math.* **44** 27
[24] Yan Z Y and Zhang H Q 2001 *J. Phys. A: Math. Gen.* **34** 1785
Barnett M P, Capitani J F, Von Zur Gathen J and Gerhard J 2004 *Int. J. Quantum Chem.* **100** 80
Xie F D and Gao X S 2004 *Commun. Theor. Phys.* **41** 353
Li B, Chen Y, Xuan H N and Zhang H Q 2004 *Appl. Math. Comput.* **152** 581
Gao Y T and Tian B 2006 *Phys. Plasmas* **13** 112901
Tian B and Gao Y T 2005 *Phys. Plasmas* **12** 054701
Tian B and Gao Y T 2005 *Phys. Lett.* A **342** 228
Tian B and Gao Y T 2006 *Phys. Lett.* A **359** 241
Tian B and Gao Y T 2007 *Phys. Lett.* A **362** 283
Tian B, Gao Y T and Zhu H W 2007 *Phys. Lett.* A **366** 223

Li J, Xu T, Meng X H, Yang Z C, Zhu H W and Tian B 2007 *Phys. Scr.* **75** 278
Li J, Meng X H, Xu T, Zhang Y X, Zhang H Q and Tian B 2007 *J. Math. Anal. Appl.* DOI:10.1016/j.jmaa.2007.03.064
[25] Tian B, Wei G M, Zhang C Y, Shan W R and Gao Y T 2006 *Phys. Lett.* A **356** 8
[26] Lou S Y and Hu X B 1998 *Commun. Theor. Phys.* **29** 145
[27] Cao C W, Wu Y T and Geng X G 1999 *J. Math. Phys.* **40** 3948
[28] Geng X G, Wu Y T and Cao C W 1999 *J. Phys. A: Math. Gen.* **32** 3733
[29] Cao C W, Geng X G and Wang H G 2002 *J. Math. Phys.* **43** 621
[30] Cheng Y and Li Y S 1991 *Phys. Lett.* A **157** 22
[31] Dai H H and Geng X G 2000 *J. Math. Phys.* **41** 7501
[32] Li Y S, Ma W X and Zhang J E 2000 *Phys. Lett.* A **275** 60
[33] Li Y S and Zhang J E 2001 *Phys. Lett.* A **284** 253
[34] Golub L *et al* 1999 *Phys. Plasmas* **6** 2205